

Further Evidence for a Merger Origin for the Thick Disk: Galactic Stars Along Lines-of-sight to Dwarf Spheroidal Galaxies

Rosemary F.G. Wyse¹, Gerard Gilmore², John E. Norris³, M. I. Wilkinson², Jan T. Kley⁴, A. Koch⁵, N.W. Evans², E. K. Grebel⁵

ABSTRACT

The history of the Milky Way Galaxy is written in the properties of its stellar populations. Here we analyse stars observed as part of surveys of local dwarf spheroidal galaxies, but which from their kinematics are highly probable to be non-members. The selection function – designed to target metal-poor giants in the dwarf galaxies, at distances of ~ 100 kpc – includes F-M dwarfs in the Milky Way, at distances of up to several kpc. The stars whose motions are analysed here lie in the cardinal directions of Galactic longitude $\ell \sim 270^\circ$ and $\ell \sim 90^\circ$, where the radial velocity is sensitive to the orbital rotational velocity. We demonstrate that the faint F/G stars contain a significant population with $V_\phi \sim 100$ km/s, similar to that found by a targeted, but limited in areal coverage, survey of thick-disk/halo stars by Gilmore, Wyse & Norris (2002). This value of mean orbital rotation does not match either the canonical thick disk or the stellar halo. We argue that this population, detected at both $\ell \sim 270^\circ$ and $\ell \sim 90^\circ$, has the expected properties of ‘satellite debris’ in the thick-disk/halo interface, which we interpret as remnants of the merger that heated a pre-existing thin disk to form the thick disk.

Subject headings: Galaxy: evolution – Galaxy: stellar content – Galaxy: structure – Galaxy: kinematics and dynamics

¹The Johns Hopkins University, Dept. of Physics and Astronomy, Baltimore, MD 21218; wyse@pha.jhu.edu

²Institute of Astronomy, Cambridge University, Madingley Road, Cambridge CB3 0HA, UK; gil@ast.cam.ac.uk

³Research School of Astronomy & Astrophysics, The Australian National University, Mount Stromlo Observatory, Cotter Road, Weston, ACT 2611; jen@mso.anu.edu.au

⁴Institute for Astronomy, University of Hawaii, 260 Woodlawn Drive, Honolulu, HI 96822; kley@ifa.hawaii.edu

⁵Astronomical Institute of the University of Basel, Department of Physics & Astronomy, Venusstr. 7, CH-4102 Binningen, Switzerland; koch@astro.unibas.ch, grebel@astro.unibas.ch

1. Introduction

The Milky Way Galaxy, once apparently satisfactorily described by Population I and Population II, is clearly a very complex system (Freeman & Bland-Hawthorn 2002). Substructure in kinematics and in coordinate space indicates accretion of (formerly) satellite galaxies (e.g. the Sagittarius dwarf spheroidal: Ibata, Gilmore & Irwin 1994; Ibata et al. 1997; Majewski et al. 2003) and disruption of star clusters (e.g. Odenkirchen et al. 2003). Merger and assimilation of satellite galaxies is an inherent part of the formation of large galaxies, like the Milky Way, in the now-canonical Λ -Cold-Dark-Matter cosmological models. Indeed thick disks of spiral galaxies are most probably relics from an early merger of the evolving thin disk and a smaller satellite galaxy (see Wyse 2005 for a recent discussion of the possibilities), and thus contain unique clues about the early stages of disk galaxy formation.

Models of the formation of thick disks through heating of a thin disk by (dissipationless) mergers usually invoke a satellite of 10-20% of the mass of the (pre-existing) stellar disk (e.g. Velaquez & White 1999; Walker, Miros & Hernquist 1996). The outer parts of the satellites are removed by tidal forces, limited by the relative densities of the satellite and larger system (essentially a Roche-Jacobi criterion). The fate of this debris has been largely ignored in the models, but it is clear that material stripped by tidal forces continues on orbits close to that of the center of mass of the satellite at the time of removal. Thus, for typical satellite/subhalo initial orbital angular momentum that is close to half that of a circular orbit of the same energy (e.g. Benson 2005; Zentner et al. 2005) one would expect an azimuthal streaming velocity of around 100km/s for satellite debris in a system like the Milky Way with a flat rotation (circular velocity) curve, with amplitude ¹ ~ 220 km/s. Identification of this satellite debris would provide strong evidence for a merger history of the thick disk.

First indications of a population that could be ascribed to debris from the satellite whose merger caused the thick disk was presented by Gilmore, Wyse & Norris (2002; hereafter GWN). This population was identified in a survey of faint (apparent V-band magnitude $V \gtrsim 18$) F/G stars in two lines of sight at intermediate latitude, at longitude $\ell \sim 270^\circ$. The primary signature was kinematics distinct from those of the canonical thick disk, and distinct from the stellar halo, with mean azimuthal streaming velocity ~ 100 km/s. Further analysis (Norris et al. 2006) has derived a characteristic metallicity about a factor of ten below the canonical thick disk, and more characteristic of stars in dwarf galaxies. But is

¹Of course in hierarchical clustering models the potential well of the Milky Way is not fixed, but observations constrain the bulk of the merging for normal galaxies to happen very early (e.g. Glazebrook et al. 2004; Unavane, Wyse & Gilmore 1996; Wyse 2005), and theory predicts an early epoch of massive mergers (e.g. Zentner & Bullock 2003).

this a pervasive population, reasonably well-mixed as expected if indeed it resulted from a merger that took place many Gyr ago?

2. Stars in Lines-of-Sight to selected Dwarf Galaxies

A side benefit of the recent effort to obtain detailed internal kinematics across the face of local dwarf spheroidal (dSph) galaxies is reasonably large samples of ‘contaminating’ stars in the Milky Way, along the line-of-sight to the target dwarf galaxy. The cardinal longitudes $\ell \sim 270^\circ$ and $\ell \sim 90^\circ$, where the radial velocity is most sensitive to azimuthal velocity (and hence orbital angular momentum, given a distance), are of particular importance. We here analyse the non-member stars from our large surveys of the Draco dSph ($\ell = 86^\circ$, $b = +35^\circ$), the Ursa Minor dSph ($\ell = 104^\circ$, $b = +45^\circ$), and the Carina dSph ($\ell = 260^\circ$, $b = -23^\circ$). The data were taken, in order of sample size, from surveys with the VLT/FLAMES, WHT/WYFFOS and Keck/HIRES, and have typical radial velocity errors of less than 3km/s.

The stars that were observed were selected from color-magnitude diagrams of each dSph to be giants at the distance of that galaxy, with a bright magnitude limit of $V \sim 17$ and faint limit of $V \lesssim 20$, with a mild trend, following the giant branch, that fainter stars are bluer. The surveys of the Draco dSph and the UMi dSph are described in Wilkinson et al. (2004), while that of the Carina dSph is described in Wilkinson et al. (2006) and in Koch et al. (2006). In general dSph have low velocity dispersions, ~ 10 km/s, and our membership probabilities were based on iterative Gaussian fitting to the radial velocity distributions. The member, and non-member, stars for each line-of-sight are shown in the color-radial velocity plane in Fig. 1. The non-members are expected to be predominantly dwarf stars within the Milky Way at typical distances of a few, to several, kiloparsec. As may be seen in the Figure, in the Draco dSph line-of-sight the member stars are well-separated from the field stars but for the Carina and UMi dSph lines-of-sight we may well have incorrectly assigned a small number of actual field stars as high-probability galaxy members. In the analysis below, this would result in a (small) deficit of stars in the Carina line-of-sight with azimuthal streaming velocity $V_\phi \sim 0$ km/s and in the UMi line-of-sight a (small) deficit of stars with $V_\phi \lesssim -150$ km/s. There is no *a priori* kinematic selection bias in the non-member stars.

3. Azimuthal Streaming Velocity

The lines-of-sight are ideal to probe the orbital angular momentum of the Galactic stars. Defining V_{helio} to be the heliocentric radial (line-of-sight) velocity of a given star,

then with V_{Gal} being the Galactocentric radial velocity of a given star, i.e. the component of the star’s Galactocentric velocity along the line-of sight from the Sun to the star, we have $V_{Gal} = V_{helio} + v_{pec,\odot,(\ell,b)} + 220(\text{km/s}) \sin \ell \cos b$. The second term here is the component of the Sun’s peculiar motion in the line-of-sight to the star, and we have assumed that the LSR has a circular orbit of 220 km/s about the Galactic Center. We adopted a solar peculiar motion of 15.4 km/s in the direction of $(\ell, b) = 51^\circ, 23^\circ$. V_{Gal} may then be decomposed as $V_{Gal} = \alpha V_r + \beta V_\phi + \gamma V_\theta$, where the coefficients are functions of Galactocentric distance plus angular coordinates, and are defined in equations 3-7 of Morrison, Freeman & Flynn (1990; hereafter MFF). With the assumption of zero means in the r and θ motions, V_{gal}/β for a given star is an unbiased estimate of V_ϕ . For example, for a solar distance of 3 kpc (a typical derived value below), $V_{Gal,Carinalos} = 0.48V_r - 0.81V_\phi + 0.33V_\theta$, $V_{Gal,Dracolos} = 0.31V_r + 0.80V_\phi - 0.52V_\theta$, and $V_{Gal,UMilos} = 0.49V_r + 0.62V_\phi - 0.61V_\theta$.

Implementation of these formulae requires distances. We utilised two isochrones from Bergbusch & Vandenberg (2001), with color-effective temperature relations from Vandenberg & Clem (2003), and assumed that the stars are main sequence dwarfs (we discuss possible subgiant contamination in section 4 below). We adopted the $V-I$, M_V relation corresponding to 12 Gyr old populations with $[\alpha/\text{Fe}] = +0.3$ and firstly $[\text{Fe}/\text{H}] = -0.525$ and secondly $[\text{Fe}/\text{H}] = -1.525$. The first was chosen since it corresponds to a large fraction of local thick disk stars (Bensby et al. 2005), while the second was chosen since this metallicity corresponds to the stars with intermediate kinematics from GWN, as well as to the ‘metal-weak thick disk’ (e.g. MFF; Chiba & Beers 2000) and to the stellar halo. Individual distances cannot be taken as reliable, but the overall derived distributions should be representative. The reddenings in the lines-of-sight of interest are all small, $E(B - V) \lesssim 0.05$ (Schlegel et al. 1998), and are ignored in the analysis. The derived distances for the vast majority of the stars are less than 5 kpc, with a typical distance being 2–3 kpc. At the faint magnitudes we analyse below, the redder stars are most likely to be in the thin disk – thick disk interface, with the bluer ones in the thick disk – halo interface.

Carina Line-of-Sight, $\ell = 260^\circ, b = -23^\circ$:

The line-of-sight to the Carina dSph contains the largest sample of non-member stars, 619 stars with apparent magnitudes in the range $17.27 \leq V \leq 20.31$ and with color in the range $0.66 \leq V - I \leq 2.61$. The vast majority are most probably normal disk stars. We here are most interested in the bluer, fainter stars. We are also interested in a comparison of the derived V_ϕ distributions in the three dwarf spheroidal lines-of-sight, and this is facilitated with a similar color range for all three. We therefore pruned the sample to the 89 stars with $19.0 < V \leq 20.0$ and with color in the range $0.90 < V - I \leq 1.1$. The Carina input sample was derived from the $V, B - V$ distribution, and the $V - I$ selection here was adopted to

compare with the other two lines-of-sight, which utilised the $V, V - I$ distribution. The histogram of derived individual estimates of $V_\phi = V_{Gal}/\beta$ for this ‘G star sample’ is shown in Figure 2, for each of the two isochrones, together with the distribution in the $V, V - I$ plane. Note that the bin size, 20 km/s, is chosen to provide significant numbers of stars per bin, and is more than four times the line-of-sight velocity uncertainty. The narrow peak at ~ 200 km/s, with the shoulder at ~ 150 km/s is due to the thin disk plus canonical thick disk (see Table 1). There is a rather high tail through $V_\phi \sim 100$ km/s, towards $V_\phi \sim 0$ km/s. These results are insensitive to the adopted metallicity (compare the solid and dashed histograms in the figure).

The thick disk/halo interface, of most interest to probe satellite debris, is best probed by the stars with $V - I \leq 0.9$. Figure 3 shows the velocity histogram of these 49 stars (all fainter than $V = 18$) compared with the 1043 stars (also $V \geq 18, V - I \leq 0.9$) in the field at $\ell \sim 270, b \sim +33$ that formed part of the sample of GWN. Given the difference in latitude, and the resultant difference in projection of V_ϕ into the line-of-sight, the agreement is good.

Draco Line-of-Sight, $\ell = 86^\circ, b = +35^\circ$:

The 207 non-member stars in this line of sight cover the apparent magnitude range $17.00 \leq V \leq 19.88$, and colors as shown in Fig. 1. We selected a ‘G-star sample’ consisting of the 82 stars with $18.25 < V \leq 19.75$ and with color in the range $0.90 < V - I \leq 1.1$. Their derived V_ϕ distribution is shown in Fig. 2, again with the $V, V - I$ color-magnitude diagram (the effects of the selection of stars following the locus of a red giant branch have not been entirely removed by these cuts). The histograms are similar to those in the Carina line-of-sight, except that the narrow peak is at the canonical thick disk mean $V_\phi \sim 170 - 180$ km/s. Again the results are insensitive to the metallicity of the adopted isochrones. This agreement with the Carina line-of-sight and the earlier GWN data is all the more important since this Draco line-of-sight is at opposite Galactic longitude, $\ell = 90^\circ$ as opposed to $\ell = 270^\circ$.

UMi Line-of-Sight, $\ell = 104^\circ, b = +45^\circ$:

The 105 non-member stars in this line of sight cover the apparent magnitude range $16.59 \leq V \leq 19.86$, with $V - I$ distribution shown in Fig. 1, We again selected a ‘G-star sample’, this time consisting of the 42 stars with $17.75 < V \leq 19.75$ and again with color in the range $0.90 < V - I \leq 1.1$. Their derived V_ϕ distribution and CMD are shown in Fig. 2, (again the effects of the initial selection of red giant stars in the dSph have not been entirely removed by these cuts). The effects of small number statistics limit the interpretation of the histograms but the distribution is clearly rather broad. Once more the results are insensitive to the metallicity of the adopted isochrones. Again, we note that this UMi line-of-sight is at Galactic longitude $\ell = 90^\circ$, as opposed to $\ell = 270^\circ$.

4. Comparison with Expectations

A direct comparison of the velocities with predictions is not trivial due to the non-standard selection function of the samples, which were chosen for reasons having nothing to do with studying the Galaxy. However, the narrower color range of the ‘G-star’ samples alleviates this to some extent (and was chosen with a model comparison in mind). Assuming uniform sampling across the color-magnitude ranges selected, each of the ‘G-star’ samples in the Draco and UMi lines-of-sight should, from the Gilmore star-count model (Gilmore 1981), be a mix of thin disk, thick disk and halo in the ratio $\sim 0.1 : 1 : 0.2$. This is consistent with the derived distances, which correspond to mean z -height above the Galactic plane of ~ 1.75 kpc for the $[\text{Fe}/\text{H}] \sim -0.5$ isochrone, and ~ 1.3 kpc for the $[\text{Fe}/\text{H}] \sim -1.5$ isochrone. The stars in the Carina line-of-sight should be a mix of $\sim 0.4 : 1 : 0.2$, again consistent with our derived mean height above the Galactic plane of 1.5 kpc for the $[\text{Fe}/\text{H}] \sim -0.5$ isochrone and 1.1 kpc for the -1.5 isochrone.

The highest statistical significance comes from the sum of all three lines-of-sight, and the lower right panel of Fig. 2 shows a simple sum of the three individual histogram, together with a model curve that is the sum of three Gaussians to represent the thin and thick disks and halo, with means and sigmas given in Table 1, in the ratios of 0.1:1:0.25 (as a compromise fit to the main thin disk/thick disk peak at ~ 190 km/s). There is a clear excess, compared to the model, of stars with $V_\phi \sim 50 - 150$ km/s. This excess is robust to rebinning (the structure around the peak at ~ 200 km/s is more sensitive). The usual Kolmogorov-Smirnoff test for comparisons of data and models is most sensitive to regions with most stars, and thus application to the entire distribution is dominated by the peak at around ~ 200 km/s, where the agreement is reasonable. We have instead applied the KS test to a restricted range of V_ϕ , finding for $V_\phi < 100$ km/s there is a 99% probability that the data are from a different distribution than the model. We obtain similar excesses at $V_\phi \sim 100$ km/s (but with lower significance due to small number statistics) from the $\ell \sim 270^\circ$ Carina line-of-sight alone, and from a sum of the $\ell \sim 90^\circ$ Draco and UMi lines-of-sight. The addition of a component with $V_\phi = 100$ km/s and $\sigma_{V_\phi} = 40$ km/s, and with normalisation equal to that of the stellar halo, greatly improves the fit.

One is required to adopt rather extreme kinematics for the canonical components of the Galaxy to avoid the addition of this extra component; for example, increasing both the thin disk and thick disk dispersions and adopting a mean rotational streaming of 30 km/s for the halo. Even with this, one cannot obtain a good fit to the distributions, but rather introduce a significant over-prediction in the model around $V_\phi \sim 150$ km/s. Vertical gradients in $\langle V_\phi \rangle$ for the thick disk have been discussed (e.g. MFF, Chiba & Beers 2000; Allende Prieto et al. 2006) but none predicts as low a value of $\langle V_\phi \rangle \sim 100$ km/s at $z < 2$ kpc.

5. Discussion

There are several possible effects that could complicate the interpretation of the above analysis. First, imperfect subtraction of the several strong sky lines in the observed data could have produced spurious radial velocities at certain values set by the wavelength of the sky line. We found that the strongest spurious signal (itself weak) in the cross-correlation peak would be expected at ~ -145 km/s and $\sim +240$ km/s, far from our reported signal.

We assumed that all stars were dwarfs when estimating distances. For the isochrones we adopted, subgiants with $V-I \sim 0.9$ are some 2–3 magnitudes brighter in the V-band than are the main sequence stars of the same color. At the apparent magnitudes of interest, subgiants would lie at distances of 10–15 kpc. The resultant deprojections of the line-of-sight velocity into V_ϕ would shift the peak at ~ 200 km/s (see Fig. 2) to $\gtrsim 300$ km/s, incompatible with all other surveys of the thick disk – thin disk interface. The $V_\phi \sim 200$ km/s peak contains stars of all colors, as does the velocity range around ~ 100 km/s, as may be inferred from Fig. 1 (remembering the typical $|\beta| \sim 0.8$). Clearly subgiant contamination must be minor, in line with the expectations from stellar evolution that this phase is short-lived compared to the main sequence, and with observed luminosity functions.

We have adopted isochrones based on our knowledge of chemical abundances in the thick-disk – halo interface, but clearly metallicity determinations for the non-member stars would be extremely useful, particularly to investigate any possible connection to the ‘metal-weak thick disk’ (e.g. Chiba & Beers 2000; MFF). This is being investigated.

6. Conclusions

We have shown that faint F/G stars, $V \gtrsim 18$, at intermediate latitudes, consistently show a population with mean azimuthal streaming that corresponds to a lag behind the Sun of ~ 100 km/s. This is dissimilar to the value for the canonical thick disk and to the value for the canonical stellar halo. We selected stars in restricted ranges of color and magnitude, in both $\ell = 270^\circ$ and $\ell = 90^\circ$, so that modulo metallicities, the stars are typically at a few kiloparsecs from the Sun, and one can infer that we have found a population of intermediate angular momentum. This population is detected in a wide range of Galactic latitude and longitude. Indeed, the K-giant sample of MFF also shows indications of this population, particularly for $[\text{Fe}/\text{H}] \lesssim -1.5$ (see their Figure 7 (d) and (g)). As noted in the introduction, this mean rotational velocity is what one would expect for debris from a typical shredded satellite. The thick disk may well have been caused by the most massive merger suffered by the Milky Way since the onset of star formation in the thin disk. In this

case, the debris from the satellite implicated in this ‘minor merger’ would dominate over other debris. We propose that this is indeed the case, and interpret our observations as tracing the remains of the satellite whose merger with the Milky Way created the thick disk. We intend to make detailed comparisons with simulations of the merger process to constrain further this last significant merger of the Milky Way.

RFGW thanks the Aspen Center for Physics for hospitality. MIW acknowledges PPARC. AK and EKG acknowledge the Swiss NSF (grant 200020-105260). We thank the referee for his quick and extremely useful report.

REFERENCES

- Allende Prieto, C., Beers, T.C., Wilhelm, R., Newberg, H., Rockosi, C., Yanny, B. & Lee, Y. 2006, *ApJ*, in press (astro-ph/0509812)
- Bensby, T., Feltzing, S., Lundström, I., & Ilyin, I. 2005 *A&A*, 433, 185
- Benson, A. 2005, *MNRAS*, 358, 551
- Bergbusch, P.A. & Vandenberg, D.A. 2001, *ApJ*, 556, 322
- Chiba, M. & Beers, T.C. 2000, *AJ*, 119, 2843
- Dehnen, W. & Binney, J. 1998, *MNRAS*, 298, 387
- Freeman, K.C. & Bland-Hawthorn, J. 2002, *ARAA*, 40, 487
- Gilmore, G. 1981, *MNRAS*, 195, 183
- Gilmore, G., Wyse, R.F.G. & Norris, J.E. 2002, *ApJL*, 574, L39 (GWN)
- Glazebrook, K. et al. 2004, *Nature*, 430, 181
- Ibata, R., Gilmore, G. & Irwin, M. 1994, *Nature*, 370, 194
- Ibata, R., Wyse, R.F.G., Gilmore, G., Irwin, M. & Suntzeff, N. 1997, *AJ*, 113, 634
- Koch, A., Grebel, E.K., Wyse, R.F.G., Kleyana, J.T., Wilkinson, M., Harbeck, D., Gilmore, G. & Evans, N.W. 2006, *AJ*, in press (astro-ph/0511087)
- Majewski, S., Struckie, M., Weinberg, M. & Ostheimer, J. 2003, *ApJ*, 599, 1082

- Morrison, H., Flynn, C. & Freeman, K.C. 1990, AJ 100, 1191 [MFF]
- Norris, J.E. 1994, 431, 645
- Norris, J.E. et al. 2006, in preparation
- Odenkirchen, M. et al. 2003, AJ, 126, 2385
- Schlegel, D., Finkbeiner, D. & Davis, M. 1998, ApJ, 500, 525
- Unavane, M., Wyse, R.F.G. & Gilmore, G. 1996, MNRAS, 278, 727
- VandenBerg, D.A. & Clem, J.L. 2003, AJ, 126, 778
- Velazquez, H. & White, S.D.M. 1999, MNRAS, 304, 254
- Walker, I., Mihos, J.C. & Hernquist, L. 1996, ApJ, 460, 121
- Wilkinson, M. et al. 2004, ApJL, 611, L21
- Wilkinson, M. et al. 2006, in preparation
- Wyse, R.F.G. 2005, in *The Local Group as an Astrophysical Laboratory*, ed. M. Livio & T.M. Brown (Cambridge: Cambridge University Press)
- Zentner, A. & Bullock, J. 2003, ApJ, 598, 49
- Zentner, A. et al. 2005, ApJ, 624, 505

Table 1. Derived mean orbital rotational velocity

Population	$\langle V_\phi \rangle$ km/s	σ_{V_ϕ} km/s	Ref.
(Old) thin disk	~ 210	20	1
Canonical thick disk	~ 175	40	2
stellar halo	~ 0	100	3
debris?	~ 100	40	4

Note. — Refs: 1 - Dehnen & Binney 1998 ; 2 - MFF; 3 - Norris 1994 ; 4 - GWN and this paper.

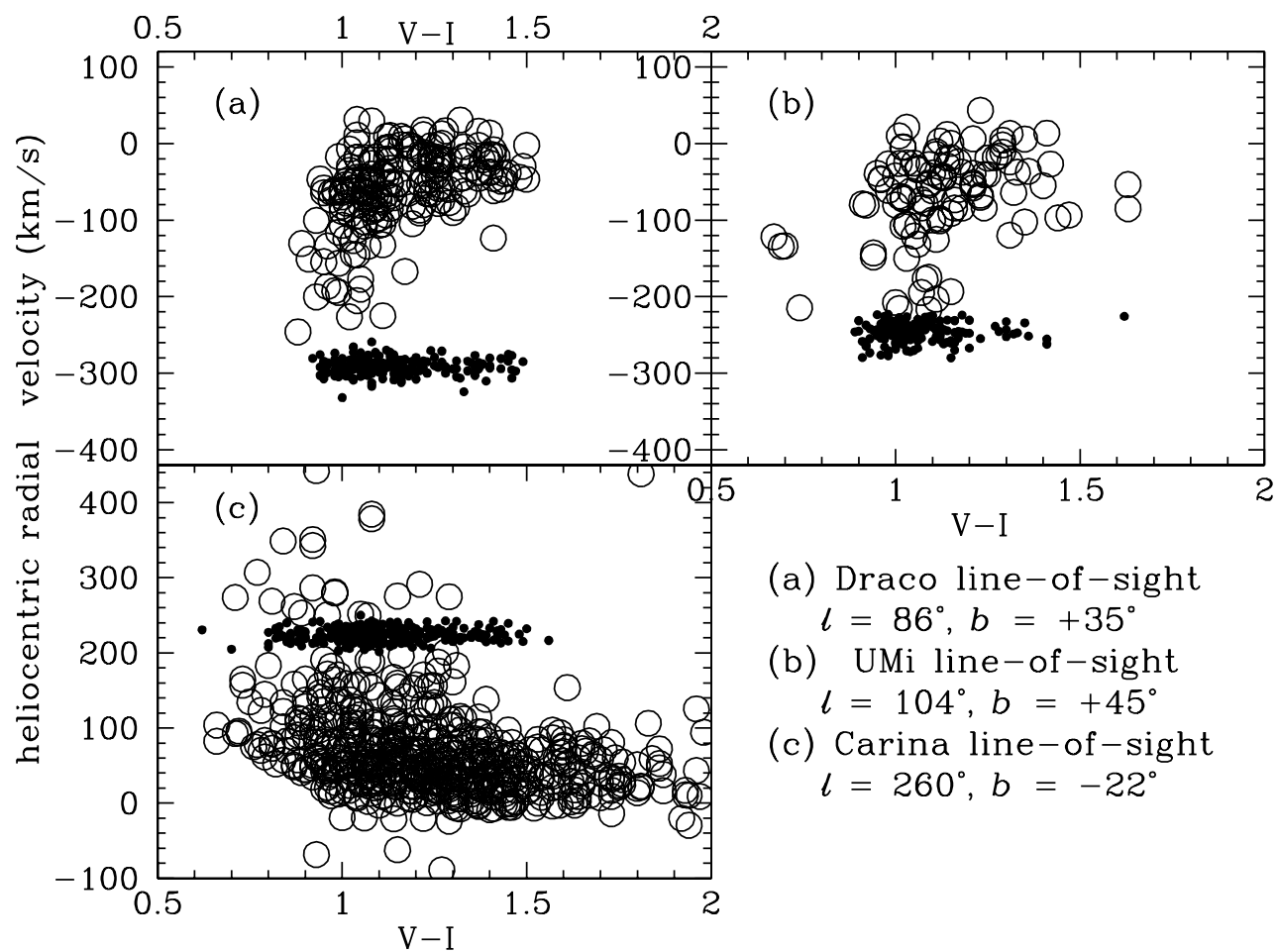


Fig. 1.— Scatter plot of V–I color versus radial velocity for all stars observed in the dwarf spheroidal lines-of-sight. Stars with very high probability to be members are indicated by small filled circles, the likely non-members are indicated by large open circles. Typical errors are a few km/s, less than the symbol size.

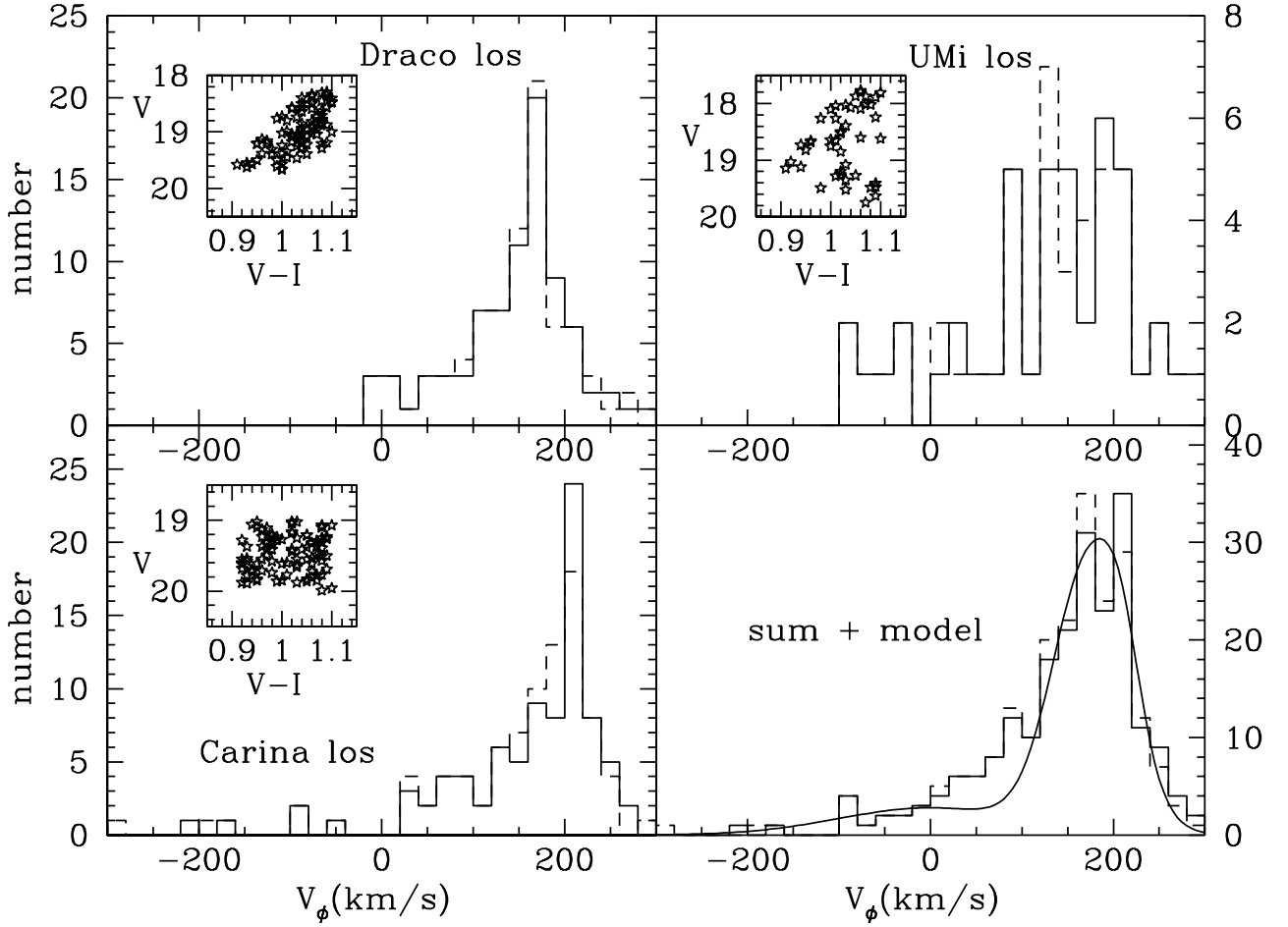


Fig. 2.— Histograms of derived azimuthal streaming velocity, $V_\phi = V_{Gal}/\beta$, for ‘G-stars’ in the three lines-of-sight to dSph, plus their V , $V - I$ distributions. The solid histograms adopt the isochrone with $[\text{Fe}/\text{H}] \sim -0.5$, while the dashed histograms adopt the more metal-poor isochrone, $[\text{Fe}/\text{H}] \sim -1.5$. The smooth curve in the lower right panel shows the expected kinematics for standard Galaxy models. The stars with derived $V_\phi \sim 100$ km/s are not expected.

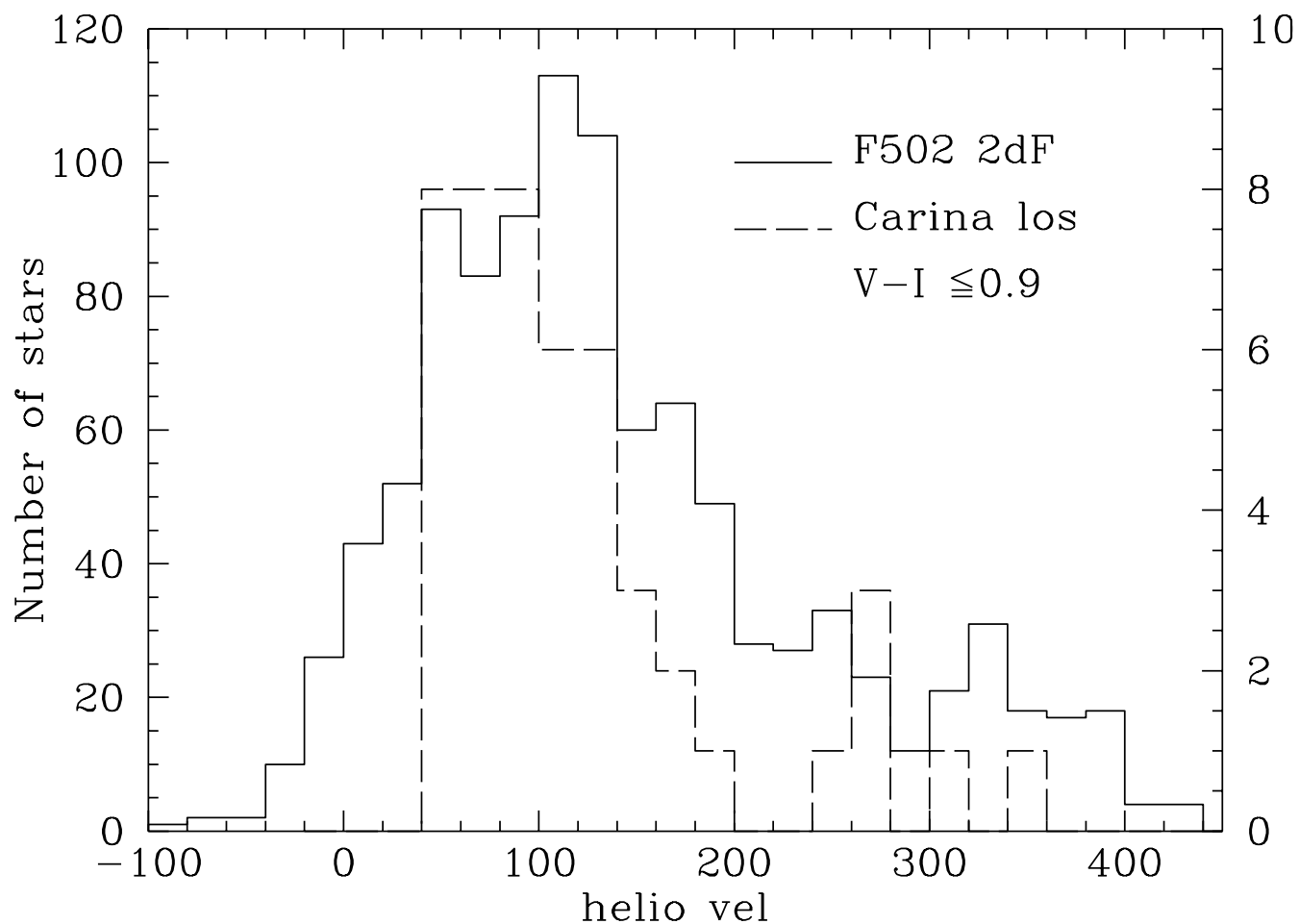


Fig. 3.— Comparison between the heliocentric radial velocity histograms for faint stars with $V \geq 18$ and that have F/G colors, in the line-of-sight to the Carina dSph ($\ell \sim 260$, $b \sim -22$) – dashed histogram, and righthand y-axis – and in field F502 ($\ell \sim 270$, $b \sim +33$). Given the difference in latitude, and the resultant difference in projection of V_ϕ into the line-of-sight, the agreement is very good.